ENVIRONMENTAL RESEARCH

LETTERS

LETTER • OPEN ACCESS

Assessing the sequestration time scales of some ocean-based carbon dioxide reduction strategies

To cite this article: D A Siegel et al 2021 Environ. Res. Lett. 16 104003

View the <u>article online</u> for updates and enhancements.

ENVIRONMENTAL RESEARCH

LETTERS



OPEN ACCESS

RECEIVED

3 April 2021

REVISED

15 June 2021

ACCEPTED FOR PUBLICATION 16 June 2021

DUDITOUED

24 September 2021

Original content from this work may be used under the terms of the Creative Commons Attribution 4.0 licence.

Any further distribution of this work must maintain attribution to the author(s) and the title of the work, journal citation and DOI.



LETTER

Assessing the sequestration time scales of some ocean-based carbon dioxide reduction strategies

D A Siegel^{1,*}, T DeVries¹, S C Doney² and T Bell³

- Earth Research Institute and Department of Geography, University of California, Santa Barbara, CA 93106-3060, United States of America
- ² Department of Environmental Sciences, University of Virginia, Charlottesville, VA 22904-4123, United States of America
- ³ Department of Applied Ocean Physics and Engineering, Woods Hole Oceanographic Institution, Woods Hole, MA 02543, United States of America
- * Author to whom any correspondence should be addressed.

E-mail: david.siegel@ucsb.edu

Keywords: ocean CO₂ removal, purposeful carbon sequestration, sequestration time scales, ocean circulation Supplementary material for this article is available online

Abstract

Ocean-based carbon dioxide (CO₂) removal (CDR) strategies are an important part of the portfolio of approaches needed to achieve negative greenhouse gas emissions. Many ocean-based CDR strategies rely on injecting CO₂ or organic carbon (that will eventually become CO₂) into the ocean interior, or enhancing the ocean's biological pump. These approaches will not result in permanent sequestration, because ocean currents will eventually return the injected CO₂ back to the surface, where it will be brought into equilibrium with the atmosphere. Here, a model of steady state global ocean circulation and mixing is used to assess the time scales over which CO₂ injected in the ocean interior remains sequestered from the atmosphere. There will be a distribution of sequestration times for any single discharge location due to the infinite number of pathways connecting a location at depth with the sea surface. The resulting probability distribution is highly skewed with a long tail of very long transit times, making mean sequestration times much longer than typical time scales. Deeper discharge locations will sequester purposefully injected CO₂ much longer than shallower ones and median sequestration times are typically decades to centuries, and approach 1000 years in the deep North Pacific. Large differences in sequestration times occur both within and between the major ocean basins, with the Pacific and Indian basins generally having longer sequestration times than the Atlantic and Southern Oceans. Assessments made over a 50 year time horizon illustrates that most of the injected carbon will be retained for injection depths greater than 1000 m, with several geographic exceptions such as the Western North Atlantic. Ocean CDR strategies that increase upper ocean ecosystem productivity with the goal of exporting more carbon to depth will have mainly a short-term influence on atmospheric CO₂ levels because \sim 70% will be transported back to the surface ocean within 50 years. The results presented here will help plan appropriate ocean CDR strategies that can help limit climate damage caused by fossil fuel CO₂ emissions.

1. Introduction

It is becoming increasingly clear that controlling future Earth warming to well below +2.0 °C and preferably +1.5 °C, as is the aim of the 2016 Paris Agreement, will require large-scale technologies to be developed that can enact negative carbon dioxide (CO₂) emissions (Fuss *et al* 2014, IPCC AR5

2014, Rogelj et al 2018). Several CO₂ removal (CDR) strategies have been proposed to provide negative emissions on global scales (NAESM 2019). These CDR strategies have been largely land-based and range from soil and forest carbon management to bioenergy with carbon capture and storage, to catalytic hydrogenation that converts CO₂ into fuels, to direct CO₂ capture and sequestration in geological

reservoirs or building materials (e.g. Fields and Mach 2017, Hepburn *et al* 2019, National Academies of Sciences, Engineering, and Medicine 2019, Fuhrman *et al* 2020).

Recently, several ocean-based CDR strategies have also been suggested. Ocean CDR approaches include enhancing the ocean's biological pump via purposeful iron additions, growing microplankton or macrophyte biomass and injecting it in the deep ocean, and rehabilitating ocean ecosystems with the aim of increasing their carbon sequestration capacity (e.g. GESAMP 2019, Gattuso et al 2021, Sala et al 2021). These strategies take advantage of biotic processes such as adding iron to stimulate photosynthesis and inorganic carbon fixation, or altering ecological food webs to increase the flux of organic matter from the surface ocean into the ocean interior (e.g. Aumont and Bopp 2006, Howard et al 2017, Sala et al 2021). Abiotic strategies have also been suggested. These include ocean alkalinization through the addition of natural alkaline materials to reduce surface seawater CO2 levels, electrochemical extraction of carbon from seawater with subsequent geological sequestration, and the direct injection of captured CO₂ from stack gases (e.g. Keller et al 2014, Renforth and Henderson 2017, Bach et al 2019). Ocean CDR strategies are popular due to the immense size of the oceans and the buffering capacity of seawater, which means that vast amounts of CO2 can be stored in the ocean interior or buried in ocean sediments. Many of these strategies also have lower social costs (sometimes referred to as win-win strategies with potentially large co-benefits) suggesting that they may be implemented more rapidly than some land-based CDR strategies (e.g. Gattuso et al 2021).

However, the ocean water column is not a permanent reservoir (e.g. Orr et al 2001, Herzog et al 2003). Subsurface water parcels where carbon is injected will eventually reach the sea surface, where the CO₂ can equilibrate with the atmosphere unless seawater alkalinity is increased to compensate for the excess CO₂. The question, then, is whether carbon injected in the ocean will interact with the atmosphere within a year, in a few decades, or on longer timescales, say O(1000) years, which is far beyond the time horizon relevant to climate policy discussions. Hence, an understanding of the timescales of purposeful ocean C sequestration is a critical component for any CDR sequestration strategy.

Here, we use an inverse ocean circulation model to assess the rate at which CO₂ that is injected into the interior ocean will leak back to the surface. We show that this leakage rate is characterized by a distribution of transit times due to the numerous fluid pathways connecting interior and surface locations in the ocean, and present metrics of this transit time distribution that provide objective measures of sequestration timescales and efficiencies for each location in the global ocean.

2. Modeling approach

The ocean circulation inverse model (OCIM) is used to simulate the leakage rate of injected CO₂ on global spatial scales. The OCIM is an offline, steady-state global ocean transport model constrained by ocean circulation tracers using an inverse approach (DeVries and Primeau 2011, DeVries 2014, DeVries and Holzer 2019). The most recent version used here has a horizontal resolution of 2° and 48 vertical levels (Holzer et al 2021). The result is the linear transport operator, T, which describes the transport of water parcels from a given model grid location with every other location in the model domain. The leakage rate of injected CO₂ is calculated by following the temporal evolution of the boundary condition propagator G(t) using the adjoint of the transport operator, T^{\dagger} , or

$$\frac{\mathrm{d}\tilde{G}}{\mathrm{d}t} = T^{\dagger}\tilde{G} \tag{1}$$

subject to the initial condition of G = 1 at the sea surface at t = 0, and the boundary condition $\tilde{G} =$ 0 at the sea surface for t > 0. This calculation is equivalent to that for determining the first passage transit time distribution (Primeau 2005). G(t) represents the distribution of times for a collection of fluid elements in the interior ocean to make next contact with the surface ocean. Note that the distribution of interior-to-surface transit times, which is the distribution that is relevant for ocean carbon sequestration, is not the same as the more commonly used surface-to-interior transit time, or ventilation age. The tracer G(t) essentially follows the evolution of the total inventory of injected CO₂ remaining in the ocean under the assumption that all of the added CO₂ reaching the ocean surface layer is rapidly removed due to air-sea gas exchange.

We calculate several metrics from $\tilde{G}(t)$ in order to characterize carbon sequestration efficiency. First, we determine the median sequestration time or median time of $\tilde{G}(t)$, the time at which 50% of the injected CO_2 remains in the interior ocean. We also calculate the mean sequestration time, which is the first moment of $\tilde{G}(t)$. Last, we assess the fraction, f(t), of injected CO_2 that remains sequestered in the interior

ocean after
$$t$$
 years (i.e. $f(t) = 1 - \int_{0}^{t} \tilde{G}(t') dt'$).
Two basic injection strategies will be explored,

Two basic injection strategies will be explored, attempting to mimic two basic modes of ocean CDR. The first is the direct injection of CO₂ or organic matter at a fixed location and depth. The second is a release of sinking organic matter following an enhancement of the biological carbon pump. This scenario is modeled by applying a sinking flux throughout the water column that follows the so-called Martin curve (Martin *et al* 1987),

$$F(z) = F(z_{\text{eu}}) \times (z_{\text{eu}}/z)^b$$
 (2)

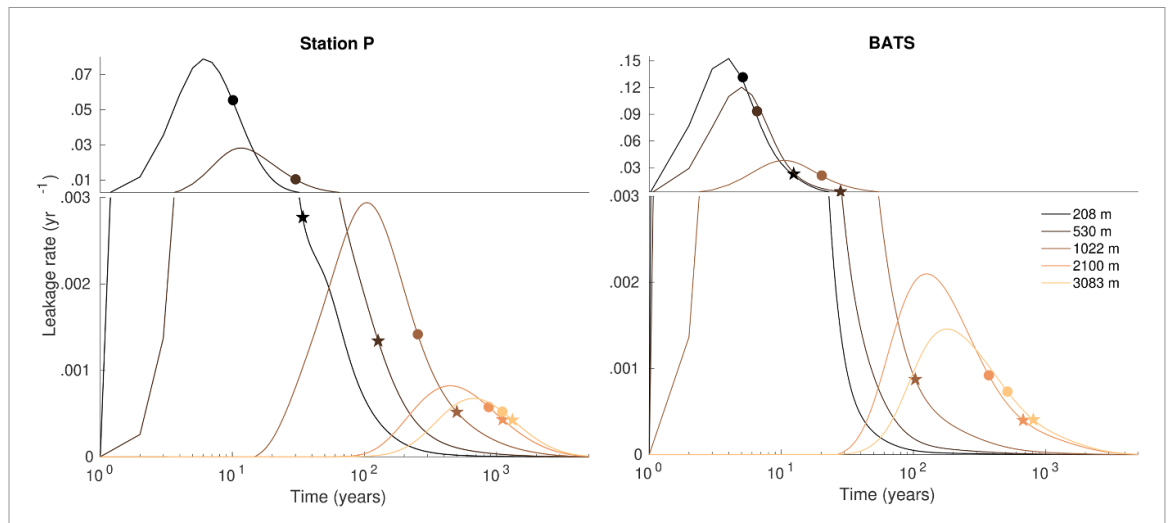


Figure 1. Leakage rate of injected CO_2 , $\tilde{G}(t)$, as a function of time since injection for five different depths at two canonical open ocean locations in the Northeast Pacific Ocean (left; Station P; 50° N 145° W) and in the Sargasso Sea in the Western North Atlantic (right; BATS; 32° N 64° W). Locations of the two sites are shown in figure 3 as the 'P' and 'B' letters for Station P and BATS, respectively. Stars give the mean sequestration time while circles represent the median sequestration time. The time integral of $\tilde{G}(t)$ over all times is equal to one by definition. Depths are the mean layer depths in OCIM.

where F(z) is the flux of the sinking carbon as a function of depth (z), $z_{\rm eu}$ is the depth of the euphotic zone (here set to 100 m), and b is the power law exponent (where b equal to 0.8 is a typical value; Buesseler et al 2007). F(z) is set to zero at the seafloor assuming complete remineralization of material sinking to the bottom and thus no sediment burial. The vertical divergence of the sinking flux is used to calculate the injection rate of CO_2 throughout the water column. Together these two approaches enable sequestration time scales to be evaluated in a consistent manner for both inputs at specific locations and depths as well as for purposeful enhancements of the biological pump.

3. Results

Modeled CO₂ leakage rates show a wide range of possible sequestration times for a given location and depth (figure 1). Shown here is the leakage rate G(t)for five different depths at two canonical locations in the Subarctic North Pacific Ocean (Station P), and in the Sargasso Sea in the western subtropical North Atlantic Gyre (Bermuda Atlantic Time series (BATS)). The distribution of $\tilde{G}(t)$ is highly positively skewed with many short times and fewer longer ones. The wide spread is due to the infinite number of pathways connecting a location at depth and the sea surface, such that some of the injected CO₂ will be relatively rapidly returned to the surface, whereas some of the CO₂ will be sequestered in the interior ocean for much longer, reaching >1000 years in the deep ocean. It should be noted that figure 1 is presented in a logarithmic scale and even then, it is positively skewed compared with a log-normal distribution. Thus, the mean of the leakage rate distribution

is much longer than the mode or median of the distribution. For example, the mode of $\tilde{G}(t)$ at 208 m at Station P is six years and its median value is ten years, while the mean sequestration time is \sim 32 years. Similar differences between mode, median and mean values of the leakage rate distribution are found for all depths for the Sargasso Sea site (BATS). Further, all three sequestration time metrics (mode, median, and mean) are substantially longer at Station P in the Subarctic North Pacific than at BATS in the Sargasso Sea. For releases centered at 1022 m, the median sequestration times at Station P are \sim 400 years compared with about 30 years at BATS.

The fraction of injected carbon that remains sequestered as a function of time, f(t), at Station P and BATS is shown in figure 2. The median sequestration time (bold black line in figure 2) illustrates how long 50% of the injected CO₂ remains sequestered. For the upper ocean at both sites (≤500 m), the median sequestration times are quite short (less than 50 years). For the Subarctic North Pacific case, these short median sequestration times extend down to ~500 m; while in the Sargasso Sea, short median sequestration times are found down to more than 1000 m. Beneath these depths, median times increase to multi-centennial scales, reaching 500 years at 1500 m at the North Pacific site and at 3000 m in the Subtropical North Atlantic. Median sequestration times greater than 1000 years are found only in the North Pacific for depths greater than 2500 m. These differences are due to differences in the overturning circulation of the Atlantic and Pacific Oceans, with the overturning bringing deep waters to the surface more rapidly in the Atlantic than Pacific Ocean. Mean sequestration times (blue bold line in figure 2) are longer than median sequestration times, with similar vertical variations.

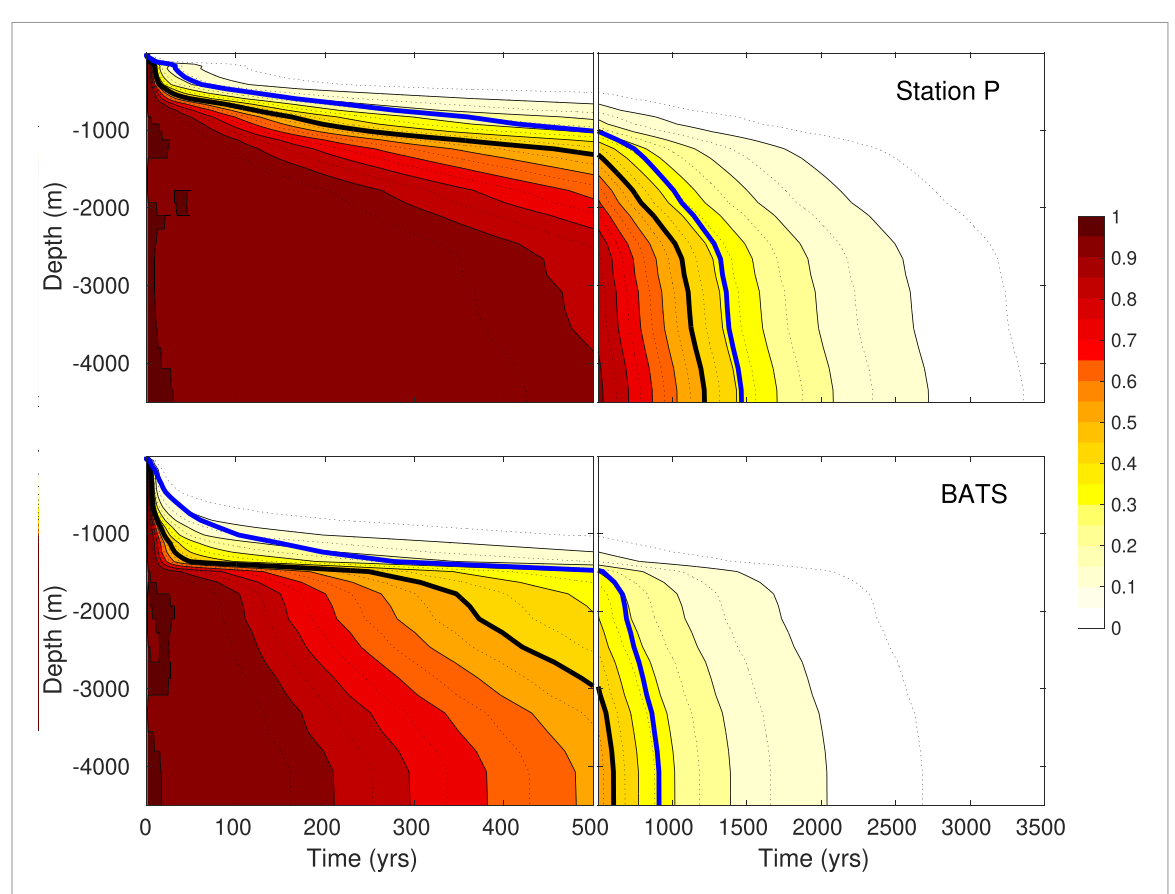


Figure 2. Fraction of discharged carbon that remains sequestered as a function of time after injection at different depths for (upper) Station P in the Subarctic Pacific and (lower) BATS in the Subtropical North Atlantic. Break between scales is at 500 years. The bold black line is the median sequestration time and the bold blue line is the mean sequestration time for CO₂ released at these depths.

The geographic variations in median sequestration times are shown in figure 3 for injection depths of 208, 530, 1022, 2100 and 3083 m. Clearly, there are large spatial differences in median sequestration times both within and between the major ocean basins. Median sequestration times are lower throughout the Atlantic and Southern Ocean basins and higher in the Pacific and Indian Oceans. For example, at the shallow discharge depths (upper 1000 m; figures 3(A)–(C)) median sequestration times are considerably shorter in subtropical gyres and the subantarctic Southern Ocean, and higher in the tropics and where bottom waters are created in the polar North Atlantic and along the Antarctic margin. Globally averaged median sequestration times are 21 years for the 208 m discharge depth and 508 years at 2100 m with extensive geographic variations (standard deviations about the global mean are 58 and 204 years for depths of 208 and 2100 m, respectively).

The distribution of the median sequestration times for purposeful enhancements of the biological pump (figure 3(E)) has similar characteristics as the upper layer (≤ 1000 m) fixed depth cases (figures 3(A)–(C)). Typical values for median sequestration time driven by biological pump enhancement range from a few decades to ~ 150 years

with a global mean value of 109 years, similar to previously estimated mean residence times of respired carbon due to the biological pump (DeVries *et al* 2012). Again, extensive spatial variations are seen (standard deviation, sd = 61 years) and median sequestration times are lower in the Atlantic and Southern Ocean basins and are considerably higher in the Pacific and Indian Oceans (figure 3(E)).

The fraction of CO₂ injected at depth that remains in the ocean after 50 years is shown in figure 4 for the two ocean CDR strategies. Figure S2 (available online at stacks.iop.org/ERL/16/104003/mmedia) shows the same quantity but for a 100 year time horizon. The injection depth is the most important variable determining how much CO₂ remains after 50 years. For shallow discharges, such as the 208 m case (figure 4(A)), only a small fraction of the injected CO₂ remains sequestered after 50 years (for the 208 m case, mean fraction = 15%, sd = 16%). At 530 m, some regions such as the western North Atlantic have lost almost all carbon after 50 years, while other regions such as the eastern tropical Pacific and the northern Indian Ocean retain nearly all carbon after 50 years (figure 4(B)). Most CO₂ injected at 1000 m will be sequestered longer than a 50 year time horizon, with few exceptions in the western North Atlantic and the Agulhas Current region in the southwest Indian

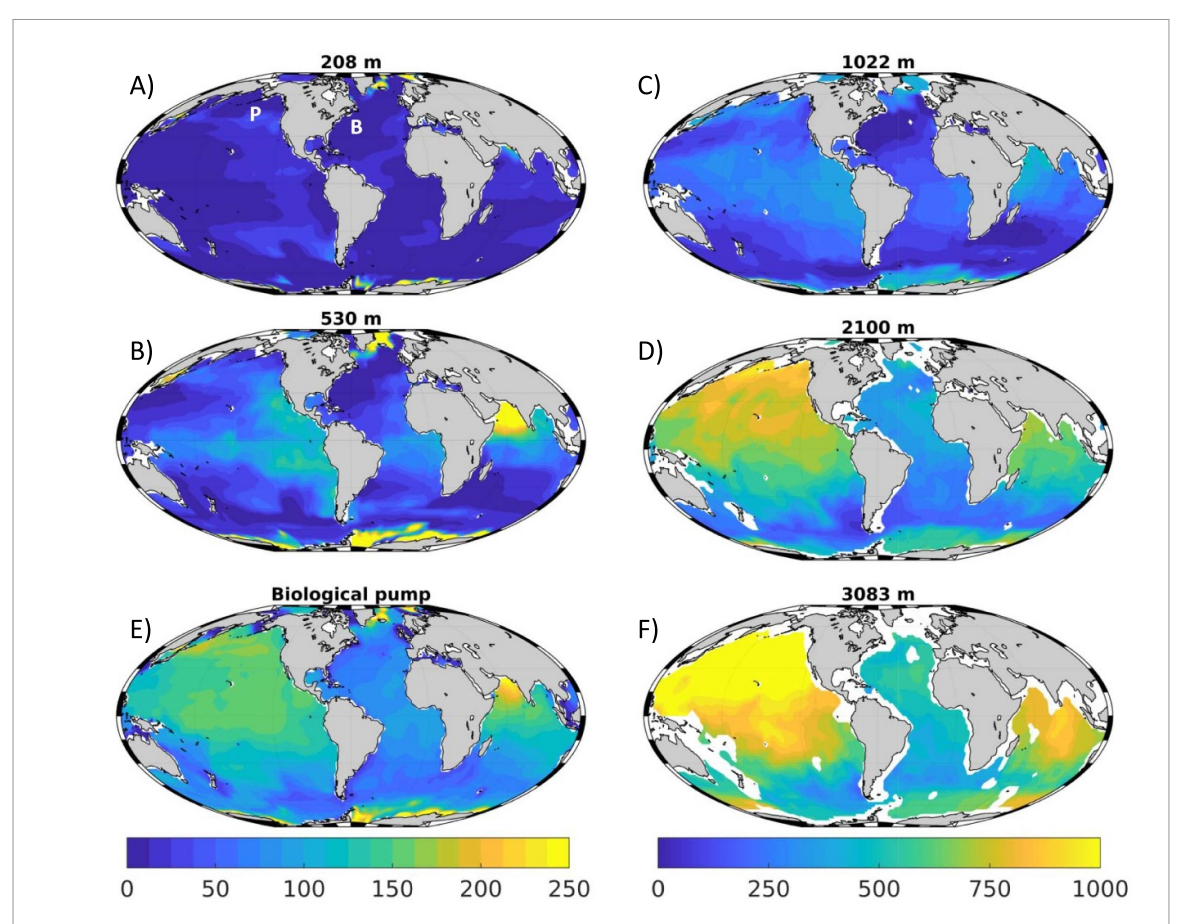


Figure 3. Geographic variation in median sequestration times for injection depths of (A) 208, (B) 530, (C) 1022, (D) 2100 and (F) 3083 m and (E) is the case where the injection follows a Martin curve remineralization profile with a power law exponent of 0.8. The left color bar is used for left column of panels while the right color bar is used for right panels. Locations of the Station P and BATS sites are shown in (A) as the white 'P' and 'B' letters, respectively.

Ocean where over 50% of CO₂ has been lost after 50 years (figure 4(C)). At a depth of 2100 m, more than 95% of the material remains sequestered after 50 years, except along the Antarctic Polar Front in the Southern Ocean where deep upwelling occurs (figure 4(D)). At 3000 m depth, essentially 100% of the CO₂ is retained after 50 years (figure 4(F)). These results provide useful guidelines for where carbon inputs should be placed to enable effective ocean-based CDR. Injecting CO₂ at the seafloor almost ensures its complete sequestration over both 50 and 100 year time scales, with exceptions where bottom waters in the Southern Ocean are created and along continental margins (figures S3(E) and (F)).

Ocean CDR strategies that increase ocean productivity and export from the upper ocean are significantly leaky when viewed over a 50 year time scale (figure 4(E)). Retention of materials input into the ocean following a Martin curve varies from \sim 20% to 50% with a global mean value of 32%, indicating that roughly two-thirds of the injected CO₂ is lost within 50 years. Again, spatial variations are apparent about this mean value (sd = 13%) with the highest retention in the Eastern Pacific and the northern Indian Ocean. After 100 years (figure S2), the retention fraction is smaller still (mean = 25% and sd = 11%), but notably the fraction lost during the first 50 years after

injection is much greater than the fraction lost in the next 50 years. These results suggest that ocean CDR strategies that aim to increase upper ocean ecosystem productivity for the goal of exporting carbon to the deep ocean will have mainly a short-term influence on atmospheric CO₂ levels.

4. Discussion

There are several important points to make about the modeled sequestration times as applied to assessing the efficacy of ocean CDR strategies. First, median sequestration times are typically many decades to centuries—not millennia except for where carbon is injected to the abyss. Second, deeper discharge depths are better than shallow ones. Hence, discharge depths of less than 500 m will likely be inefficient as typical median sequestration times at these depths are far less than 100 years. This is especially relevant for ocean CDR strategies that enhance the marine biological pump because a large fraction of the resulting export flux of organic carbon will be remineralized to CO₂ above 500 m depth. Third, geographic location is important as there are large differences in sequestration time metrics within and between ocean basins. Last, the sequestration time distribution of the leakage rate is highly skewed, such that the median

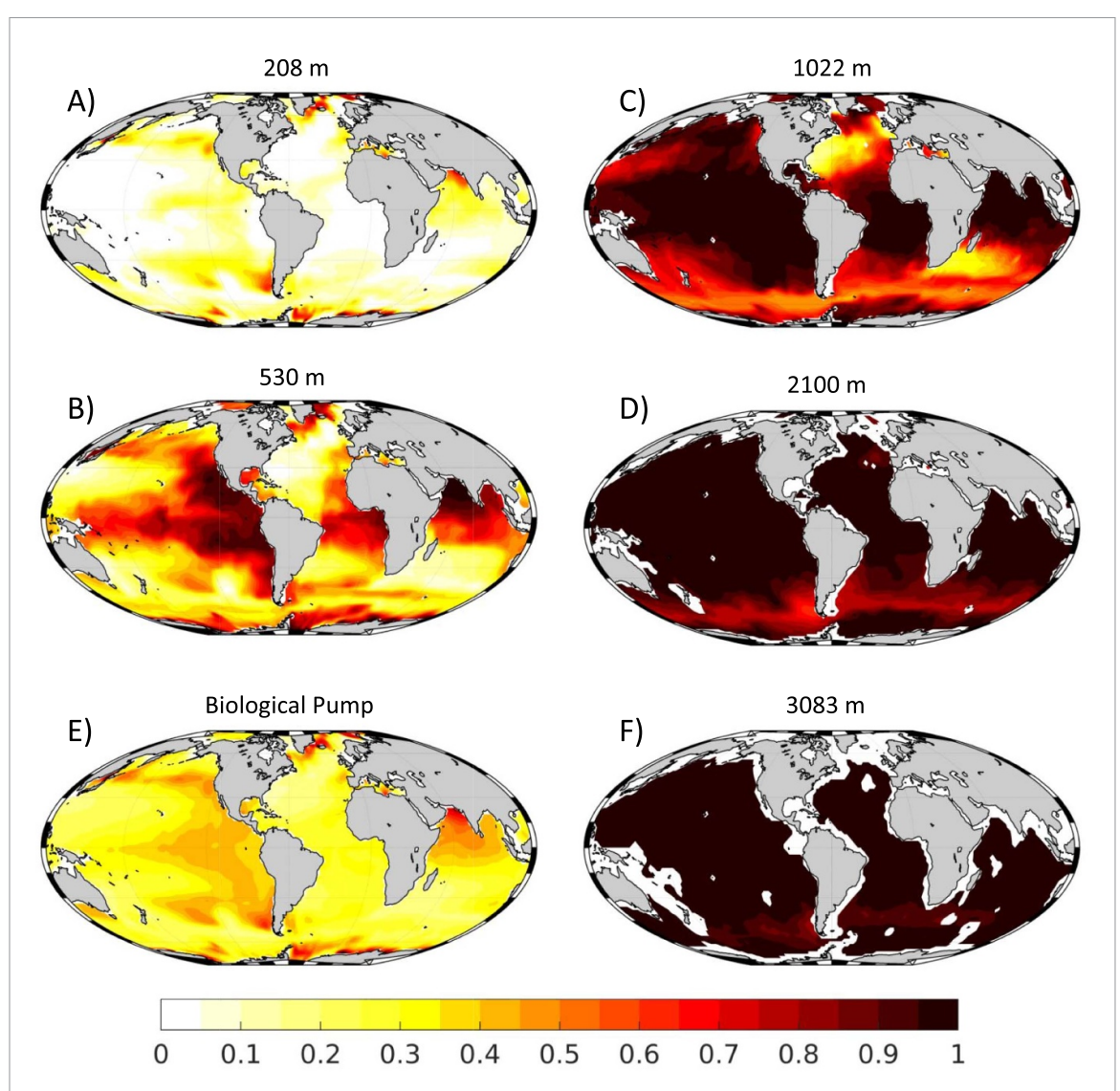


Figure 4. Maps of the fraction of CO_2 retained after 50 years for injection depths of (A) 208, (B) 530, (C) 1022, (D) 2100 and (F) 3083 m and (E) the biological pump enhancement case where the injection follows a Martin curve profile with a power law exponent of 0.8.

and mean sequestration times are much higher than the modes of these distributions. This means that the leakage of sequestered carbon evaluated over typical planning horizons (50–100 years) is often the dominant fraction of the amount injected for depths <500 m. These considerations all point to the need to plan appropriately so that ocean CDR strategies can be implemented that will successfully sequester carbon on appropriate timescales.

4.1. Considerations

There are many considerations that need to be acknowledged associated with the modeling performed and its application for assessing the permanence of ocean CDR strategies. The OCIM is a large-scale (\sim 200 km), steady state inverse model that is constrained by physical and transient oceanographic tracer data. The current suite of physical circulation tracers, such as chlorofluorocarbons (assimilated by the OCIM), tritium- 3 He and bomb-radiocarbon

(not assimilated by the OCIM), provide relatively strong constraints on ocean ventilation (transport from surface to the interior). Uniquely, the OCIM also assimilates mantle ³He and natural radiocarbon, which are among the few tracers that can be used to constrain the transport from interior to surface (DeVries and Holzer 2019), which would be relevant to ocean CDR sequestration efficiency. The OCIM has also been shown to accurately model the distribution of biogeochemical tracers such as nutrients and oxygen (DeVries et al 2013, DeVries and Weber 2017, Roshan et al 2020). However, due to its coarse spatial resolution and lack of temporal variability, the model does not capture the dynamics of coastal regions and surface mixed layers. Nonetheless, both of these oceanic regimes experience enhanced mixing rates, and in the case of the coastal ocean the seafloor is relatively shallow. Thus, these locations will not contribute to long sequestration times for carbon that is injected into the water column.

The present analysis is aimed at assessing the degree of permanence of two basic CDR strategies; the direct injection of CO₂ or rapidly oxidized carbon-rich organic matter at a fixed location and depth (including the seafloor), and the purposeful enhancement of upper ocean productivity to enhance the biological pump. The present analysis will not apply to other proposed ocean CDR strategies, such as strategies that change seawater chemistry by artificial alkalinization (e.g. Renforth and Henderson 2017, Bach *et al* 2019), or strategies that lead to the permanent burial of organic carbon in seafloor sediments.

We are also not considering any ecological or biogeochemical interactions with the injected carbon with the environment. For example, biological fertilization and artificial upwelling CDR approaches would alter ocean nutrient distributions, and in some situations the subsequent upwelling of these excess nutrients would support enhanced biological production downstream, limiting the loss to the atmosphere of excess CO₂. Our sequestration time calculations also assume that all injected carbon that is transported back to the sea surface instantaneously equilibrates with the atmosphere. Hence, the timescale associated with the chemical equilibration of CO_2 at the sea surface is not considered. For CO_2 , the air-sea equilibration time-scale is lengthened relative to other gases due to the buffering capacity of seawater, such that the typical CO₂ gas equilibration timescale is O(1 year) (Emerson and Hedges 2008). This is much shorter than the decadal to centennial sequestration scales presented here, and will not significantly affect sequestration times for most regions, although could be important where upwelled surface waters are subducted back into the interior relatively rapidly compared to the gas exchange equilibration time-scale, such as in the Southern Ocean (Ito and Follows 2013). Finally, the steady-state OCIM circulation does not capture the possible effects of ongoing and future climate change and increasing ocean stratification or increasing atmospheric CO₂ levels on sequestration time-scales.

4.2. Appropriate transit time distribution metrics for assessing ocean CDR strategies

Our results highlight the variable and impermanent nature of purposeful ocean carbon sequestration. In particular, the leakage of injected CO₂ occurs across a broad range of timescales that are skewed with very long tails, even when viewed on a logarithmic axis (figure 1). This results in mean sequestration times being much longer than sequestration times for either the median or mode of the distribution of occurrences. In the oceanographic literature, focus has been assessing water mass transit times applied to scalar transport for transient tracers that reset their concentrations via contact with the atmosphere, and for these objectives the mean surface-to-interior transit

time has most often been considered (e.g. England 1995, Khatiwala *et al* 2001, Primeau 2005, DeVries and Primeau 2011).

However, different metrics are needed for assessing ocean CDR strategies, which depends on the interior-to-surface transit time. The mean sequestration time is longer than the transit time for 60%–80% of the possible pathways connecting the subsurface and surface ocean (figure 2). Therefore, the median sequestration time (figure 3) is considerably less than the mean, and half of the trajectories linking the ocean interior with the surface ocean will have a transit time much less than the median value (figure 1). Hence, neither the mean nor median sequestration times are by themselves sufficient for assessing the efficacy of ocean CDR strategies.

What other metrics would be appropriate for assessing the sequestration efficiency of water column ocean CDR strategies? The fraction of CO₂ injected at depth that remains in the ocean over a planning time horizon appears to be a good candidate. Here, we have illustrated the geographic patterns expected for the retained fraction of injected CO₂ after 50 and 100 years for the two ocean CDR strategies investigated (figures 4 and S2). For sequestration strategies focused on inputs at a fixed depth, the injection depth is the most important variable determining how much CO₂ remains sequestered. Within a given injection depth strata, factor of two regional differences in the retained fractions are also apparent.

Ocean CDR strategies that increase ocean productivity and export are significantly leaky when evaluated over a 50–100 year planning horizons. Averaged over global scales, 32% of the input materials remain sequestrated after 50 years, and 25% after 100 years. Spatial variations in the retained fraction are muted compared to the fixed depth cases, but are still significant. Altering the Martin curve power law exponent in equation (2) has a bearing on the fraction of retained materials (figure S3). Using b values of 0.6 and 1.0 (the expected range in natural systems), the global mean retention fractions vary from 40% to 25% after 50 years (compared with 32% for the canonical b value of 0.8). Thus, even CDR strategies that substantially change the remineralization length scales for sinking carbon will have only a limited impact on the storage of sequestered carbon on typical planning time scales. These results suggest that any ocean CDR strategy that aims to increase upper ocean ecosystem productivity for the goal of exporting carbon to the deep ocean will have mainly a shortterm influence on atmospheric CO₂ levels (see also Aumont and Bopp 2006, Hauck et al 2016).

4.3. Are 'leaky' ocean CDR strategies useful?

Ocean CDR strategies that inject or store carbon within the water column will result in impermanent carbon sequestration due to the exchange of water parcels between depth and the surface ocean created by ocean circulation and mixing (Orr et al 2001, Herzog et al 2003, Aumont and Bopp 2006). The question arises whether these 'leaky' ocean CDR strategies could be a useful part of an ocean CDR portfolio. The effect of the leaky CDR strategies assessed here is to delay CO₂ emissions to the future. Economically, a leaky ocean CDR strategy may be useful if future CO₂ emissions are discounted relative to present ones (e.g. Herzog et al 2003). This is analogous to how life cycle assessments are used to account for the temporary nature of land-based afforestation CDR strategies (e.g. Levasseur et al 2010, Brandão et al 2013). Short-term CDR strategies can be used as insurance to buy time to enable technological decarbonization, greenhouse gas emission reduction, and other CDR advancements in the pipeline to come to fruition. Short-term CDR strategies can also help limit global environmental damages by delaying CO₂ emissions to a future date when emissions may be less devastating.

The efficiency of ocean CDR strategies can be quantified given the leakage rate of CO2, such as illustrated in figure 1, and an appropriate discount rates for future carbon emissions (e.g. Herzog et al 2003). The true sequestration benefit also depends on the marginal costs of the CDR strategy relative to other strategies and to marginal abatement costs, and the marginal damages of carbon emissions and the environmental and social impacts of the given strategy. For any CDR strategy, knowledge is needed on its energy use, resource demands, as well as a full life-cycle analysis of greenhouse gas emissions and other climate influences. Evaluation of CDR strategies also require an assessment of potential environmental impacts, including acidification, deoxygenation and eutrophication (e.g. Gruber 2011). These aspects required for evaluating the effectiveness of leaky ocean CDR strategies are beyond the scope of this present contribution; however, the sequestration time metrics presented here provide the needed data to assess the importance of leakage on the true efficacy of ocean CDR strategies.

Data availability statement

The OCIM CO₂ sequestration fractions are available in the FigShare database under accession code https://doi.org/10.6084/m9.figshare.15228690.v1.

Acknowledgments

D A S acknowledges support from NASA Grant 80NSSC17K0692. D A S and T B acknowledge support from US Department of Energy's Advanced Research Projects Agency–Energy cooperative Agreement DE-AR0000922. T D acknowledges support from NSF Grant OCE-1948955. S C D acknowledges support from the University of Virginia Environmental Resilience Institute.

ORCID iDs

D A Siegel https://orcid.org/0000-0003-1674-3055
T DeVries https://orcid.org/0000-0002-7771-9430
S C Doney https://orcid.org/0000-0002-3683-2437

T Bell https://orcid.org/0000-0002-0173-2866

References

Aumont O and Bopp L 2006 Globalizing results from ocean in situ iron fertilization studies Glob. Biogeochem. Cycles 20 GB2017

Bach L T, Gill S J, Rickaby R E, Gore S and Renforth P 2019 CO₂ removal with enhanced weathering and ocean alkalinity enhancement: potential risks and co-benefits for marine pelagic ecosystems Front. Clim. 1 7

Brandão M, Levasseur A, Kirschbaum M U, Weidema B P, Cowie A L, Jørgensen S V, Hauschild M Z, Pennington D W and Chomkhamsri K 2013 Key issues and options in accounting for carbon sequestration and temporary storage in life cycle assessment and carbon footprinting *Int. J. Life Cycle Assess.* 18 230–40

Buesseler K O *et al* 2007 Revisiting carbon flux through the ocean's twilight zone *Science* **316** 567–70

DeVries T 2014 The oceanic anthropogenic CO₂ sink: storage, air-sea fluxes, and transports over the industrial era *Glob*. *Biogeochem*. *Cycles* **28** 631–47

DeVries T, Deutsch C, Rafter P A and Primeau F 2013 Marine denitrification rates determined from a global 3D inverse model *Biogeosciences* **10** 2481–96

DeVries T and Holzer M 2019 Radiocarbon and helium isotope constraints on deep ocean ventilation and mantle-³He sources *J. Geophys. Res.* **124** 3036–57

DeVries T and Primeau F 2011 Dynamically and observationally constrained estimates of water-mass distributions and ages in the global ocean *J. Phys. Oceanogr.* 41 2381–401

DeVries T, Primeau F and Deutsch C 2012 The sequestration efficiency of the biological pump *Geophys. Res. Lett.* **39** L13601

DeVries T and Weber T 2017 The export and fate of organic matter in the ocean: new constraints from combining satellite and oceanographic tracer observations *Glob. Biogeochem. Cycles* 31 535–55

Emerson S and Hedges J 2008 Chemical Oceanography and the Marine Carbon Cycle (Cambridge: Cambridge University Press) (https://doi.org/10.1017/CBO9780511793202)

England M H 1995 The age of water and ventilation timescales in a global ocean model *J. Phys. Oceanogr.* **25** 2756–77

Field C B and Mach K J 2017 Rightsizing carbon dioxide removal Science 356 706–7

Fuhrman J, McJeon H, Patel P, Doney S C, Shobe W M and Clarens A F 2020 Food–energy–water implications of negative emission technologies in a +1.5°C future *Nat. Clim. Change* 10 920–7

Fuss S *et al* 2014 Betting on negative emissions *Nat. Clim. Change* 4 850–3

Gattuso J P, Williamson P, Duarte C M and Magnan A K 2021 The potential for ocean-based climate action: negative emissions technologies and beyond *Front. Clim.* **2** 37

GESAMP 2019 High level review of a wide range of proposed marine geoengineering techniques *Rep. Stud. GESAMP No.* 98 ed P W Boyd and C M G Vivian (IMO/FAO/UNESCO-IOC/UNIDO/WMO/IAEA/UN/UN Environment/ UNDP/ISA Joint Group of Experts on the Scientific Aspects of Marine Environmental Protection) p 144

Gruber N 2011 Warming up, turning sour, losing breath: ocean biogeochemistry under global change *Phil. Trans. R. Soc.* A 369 1980–96

Hauck J, Köhler P, Wolf-Gladrow D and Völker C 2016 Iron fertilisation and century-scale effects of open ocean

- dissolution of olivine in a simulated CO₂ removal experiment *Environ*. *Res. Lett.* 11 024007
- Hepburn C, Adlen E, Beddington J, Carter E A, Fuss S, Mac Dowell N, Minx J C, Smith P and Williams C K 2019 The technological and economic prospects for CO₂ utilization and removal *Nature* 575 87–97
- Herzog H, Caldeira K and Reilly J 2003 An issue of permanence: assessing the effectiveness of temporary carbon storage Clim. Change 59 293–310
- Holzer M, DeVries T and de Lavergne C 2021 Diffusion controls the ventilation of a Pacific Shadow Zone above abyssal overturning *Nat. Commun.* 12 1–13
- Howard J, Sutton-Grier A, Herr D, Kleypas J, Landis E, Mcleod E, Pidgeon E and Simpson S 2017 Clarifying the role of coastal and marine systems in climate mitigation *Front. Ecol. Environ.* **15** 42–50
- IPCC 2014 Climate Change 2014 Mitigation of Climate Change, Contribution of Working Group III to the Fifth Assessment Report of the Intergovernmental Panel on Climate Change ed O Edenhofer et al (Cambridge: Cambridge University Press)
- Ito T and Follows M J 2013 Air-sea disequilibrium of carbon dioxide enhances the biological carbon sequestration in the Southern Ocean Glob. Biogeochem. Cycles 27 1129–38
- Keller D, Feng E and Oschlies A 2014 Potential climate engineering effectiveness and side effects during a high carbon dioxide-emission scenario Nat. Commun. 5 3304
- Khatiwala S, Visbeck M and Schlosser P 2001 Age tracers in an ocean GCM Deep Sea Res. I 48 1423–41

- Levasseur A, Lesage P, Margni M, Deschênes L and Samson R 2010 Considering time in LCA: dynamic LCA and its application to global warming impact assessments *Environ*. Sci. Technol. 44 3169–74
- Martin J H, Knauer G A, Karl D M and Broenkow W W 1987 VERTEX: carbon cycling in the northeast Pacific *Deep Sea Res.* A 34 267–85
- National Academies of Sciences, Engineering, and Medicine 2019

 Negative Emissions Technologies and Reliable Sequestration: A

 Research Agenda (Washington, DC: The National Academies

 Press) (https://doi.org/10.17226/25259)
- Orr J C et al 2001 Ocean CO₂ sequestration efficiency from 3D ocean model comparison *GHGT-5*, *Greenhouse Gas Control Technologies* (Australia: CSIRO) pp 469–74
- Primeau F 2005 Characterizing transport between the surface mixed layer and the ocean interior with a forward and adjoint global ocean transport model *J. Phys. Oceanogr.* 35 545–64
- Renforth P and Henderson G 2017 Assessing ocean alkalinity for carbon sequestration *Rev. Geophys.* 55 636–74
- Rogelj J *et al* 2018 Scenarios towards limiting global mean temperature increase below 1.5 °C *Nat. Clim. Change*
- Roshan S, DeVries T, Wu J, John S and Weber T 2020 Reversible scavenging traps hydrothermal iron in the deep ocean *Earth Planet. Sci. Lett.* **542** 116297
- Sala E et al 2021 Protecting the global ocean for biodiversity, food and climate Nature 592 397–402